ChemPubSoc Europe

DOI: 10.1002/cmdc.201402099

Synthesis and Antisense Properties of 2′-*O*-(2*S*-Methoxypropyl)-RNA-Modified Gapmer Antisense Oligonucleotides

Jinghua Yu, Sanjay K. Pandey, Hetal Khatri, Thazha P. Prakash, Eric E. Swayze, and Punit P. Seth*[a]

To ascertain whether increasing hydrophobicity can enhance the activity of second-generation antisense oligonucleotides (ASOs) in muscle, we investigated the antisense properties of 2′-*O*-(2*S*-methoxypropyl)-RNA (2*S*-MOP)-modified ASOs. Synthesis of the 2*S*-MOP 5-methyl uridine phosphoramidite was accomplished on a multi-gram scale by Lewis-acid-catalyzed ring opening of 5′-*O*-*tert*-butyldiphenylsilyl ether-protected 2,2′-anhydro-5-methyl uridine with 2*S*-methoxy-1-propanol. Synthesis of the 2*S*-MOP 5-methyl cytidine nucleoside from the corresponding 5-methyl uridine nucleoside was accomplished by formation and displacement of a 4-triazolide intermediate with aqueous ammonia. 2*S*-MOP-modified oligonucleotides were prepared on an automated DNA synthesizer and showed similar enhancements in duplex thermal stability as 2′-*O*-methoxyethyl RNA (MOE)-modified oligonucleotides. 2*S*-MOP-containing antisense oligonucleotides were evaluated in Balb-c mice and showed good activity for decreasing the expression levels of scavenger receptor B1 (*Srb1*) and phosphatase and tensin homologue (*PTEN*) mRNA in liver and muscle tissue.

Second-generation antisense oligonucleotides (ASOs) are chimeric oligonucleotides that promote degradation of the targeted RNA through the RNase H mechanism.[1,2] These ASOs are typically fully modified with the phosphorothioate (PS, **1**)[3] linkage and have a central window of 8–16 DNA nucleotides flanked on either end with 2′-*O*-methoxyethyl RNA (MOE, **2**) nucleotides.[4] The PS linkage improves ASO metabolic stability and also enhances ASO binding to plasma proteins. This prevents the ASO from being excreted in the urine and facilitates ASO distribution into peripheral tissues.[5] The central DNA gap region serves as the substrate for RNase H, while the flanking MOE nucleotides enhance ASO affinity for complementary RNA and further stabilize the ASO from nuclease-mediated metabolism (Figure 1 A).[6] Second-generation ASOs represent the most advanced oligonucleotide therapeutic platform in the clinic. One second-generation ASO, Kynamro, was recently approved by the US Food and Drug Administration (FDA) for the treatment of familial hypercholesterolemia.[7] In addition, over 30 ASOs are at various stages of development in clinical trials for the treatment of metabolic, cardiovascular, cancer, and orphan diseases.

PS-modified gapmer ASOs generally show best activity in liver, which is the primary site of accumulation of this class of molecules.[5] However, chemical modifications that improve ASO activity in tissues, such as skeletal muscle, could be extremely useful for developing oligonucleotide-based therapeutics for the treatment of muscular dystrophies.[8] Towards this end, we recently showed that gapmer ASOs modified with hydrophobic modifications such as *S*-constrained ethyl bridged nucleic acid (BNA) (*S*-cEt, **3**)[9] or tricyclo-DNA[10] show improved antisense pharmacology in tissues other than liver.[11] To ascertain whether the antisense properties of MOE oligonucleotides in extrahepatic tissues could be similarly enhanced by increasing the hydrophobicity of the 2′-*O*-methoxyethyl substituent, we synthesized 2′-*O*-(2*S*-methoxy)-propyl RNA (2*S*-MOP, **4**) and examined the antisense properties of this and other modified gapmer ASOs (Figure 1 B).

Crystal structures of a MOE-modified RNA duplex showed that the MOE side chain is extensively hydrated and projects into the minor groove of the modified duplex.[12] As a result,

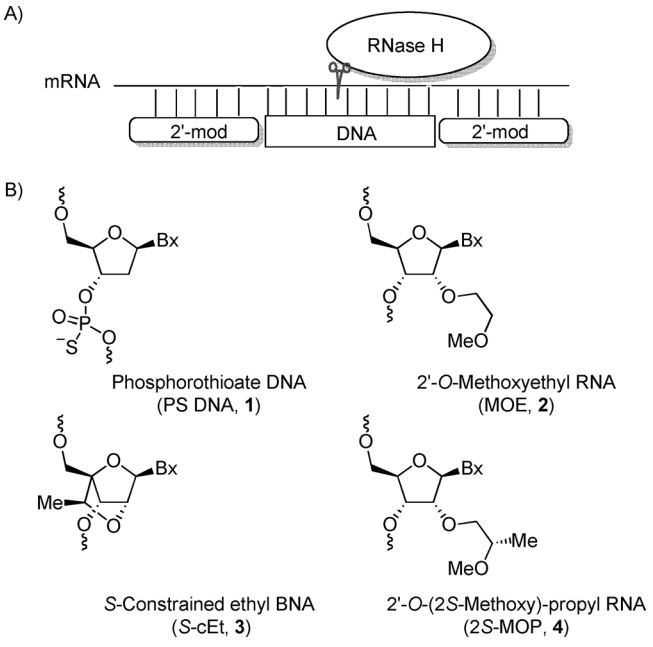

Figure 1. A) Pictorial representation of the RNase H antisense mechanism of gene silencing using 2′-modified gapmer antisense oligonucleotides (ASOs); B) Structures of PS DNA (**1**), MOE (**2**), *S*-cEt (**3**), 2*S*-MOP (**4**) nucleotides.

[a] *J. Yu, Dr. S. K. Pandey, H. Khatri, Dr. T. P. Prakash, Dr. E. E. Swayze, Dr. P. P. Seth*
Isis Pharmaceuticals, Inc.
2855 Gazelle Court, Carlsbad, CA 92010 (USA)
E-mail: pseth@isisph.com

Supporting information for this article is available on the WWW under http://dx.doi.org/10.1002/cmdc.201402099

the MOE side chain creates a sphere of hydration around the backbone PS linkage. This decreases nonspecific binding of the ASO to extra- and intracellular proteins and greatly mitigates the nonspecific toxicities of PS DNA ASOs resulting from promiscuous protein binding.[13] The crystal structure also showed that the oxygen atom of the MOE side chain exists in a gauche orientation relative to the 2′-oxygen atom on the RNA furanose ring. This interplay between the MOE side chain and the 2′-oxygen atom further rigidifies the conformation of the furanose in the C3-endo sugar pucker and improves affinity for complementary RNA.

We hypothesized that introducing a methyl group in a stereo-defined manner at the 2-position of the MOE side chain could enhance the gauche effect leading to further enhancement of RNA affinity and metabolic stability towards nuclease-mediated degradation.[14] For our initial evaluation, we decided to focus on the 2*S*-MOP isomer **4**, where the 2-methyl group was not expected to interfere with the backbone hydration and was expected to project away from the nucleobase (Figure 2).

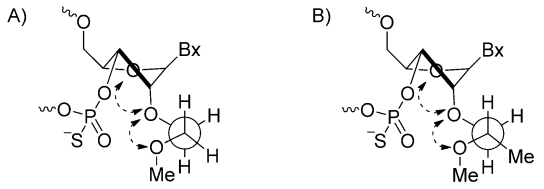

Figure 2. Structures of MOE (**2**) and 2*S*-MOP (**4**) nucleotides in the RNA-like C3′-endo conformation. A) In MOE, the gauche oxygen atoms trap water around PS backbone; B) In 2*S*-MOP, the methyl group reinforces gauche effect and increases hydrophobicity in minor groove.

The industrial-scale synthesis of MOE pyrimdine nucleosides involves a Lewis-acid-mediated ring opening of 2,2′-anhydro nucleosides, such as **5**, using methoxyethanol as the solvent.[15] This process can be conveniently carried out on a multi-kilogram scale with minimal protecting group manipulations. We envisaged using a similar strategy for the synthesis of the 2*S*-MOP thymidine nucleoside **7** (Scheme 1). We anticipated using optically pure alcohol **6** to effect ring opening of the anhydro nucleoside (**5**) in the presence of an appropriate Lewis acid. Alcohol **6** was first prepared from the corresponding commercially available ester by reduction with lithium aluminum hydride (Supporting Information).

Reaction of anhydro nucleoside **5** with alcohol **6** in the presence of trimethylaluminum as the Lewis acid provided nucleoside **7** in good yield on a 50 g scale. The *tert*-butyldiphenylsilyl ether (TBDPS) group in **7** was removed using triethylamine trihydrofluoride in THF[16] followed by re-protection of the 5′-hydroxy group as the 4,4′-dimethoxytrityl (DMTr) ether to provide nucleoside **8** in good overall yield (65% over two steps). A phosphitylation reaction provided phosphoramidite **9**, which was now ready for automated oligonucleotide synthesis.

Synthesis of the 5-Me-cytidine phosphoramidite **11** was accomplished from nucleoside **8** as shown in Scheme 2 using a slight modification of a previously described procedure.[16]

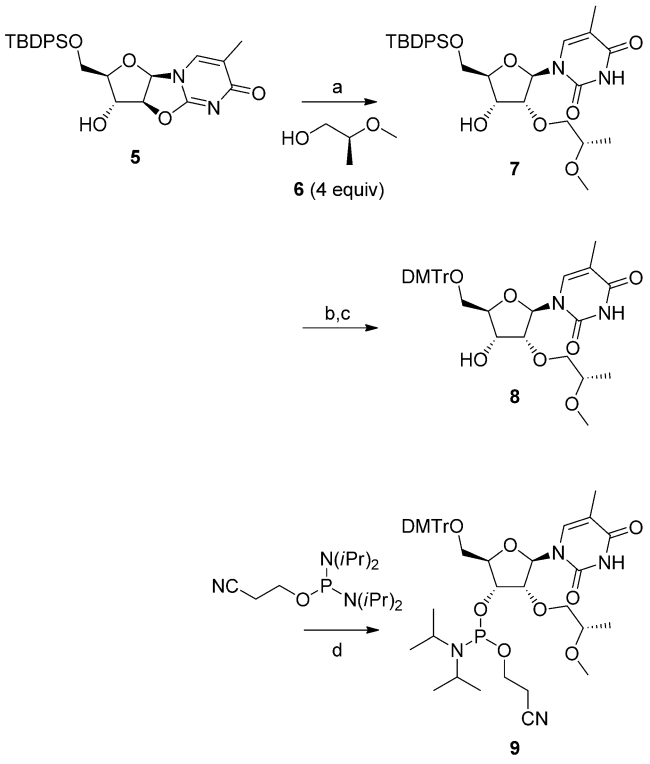

Scheme 1. Gram-scale synthesis of 2*S*-MO*P* thymidine phosphoramidite **9**. *Reagents and conditions*: a) Me_3Al in heptane (1.5 equiv), 130 °C, 66 h, pressure vessel, (42%, 50 g scale); b) $Et_3N{\cdot}3HF$, Et_3N, THF; c) DMTrCl, pyr, RT, 16 h (65%, two steps); d) *N*-methyl-imidazole (0.25 equiv), tetrazole (0.8 equiv), DMF, RT, 8 h, (85%).

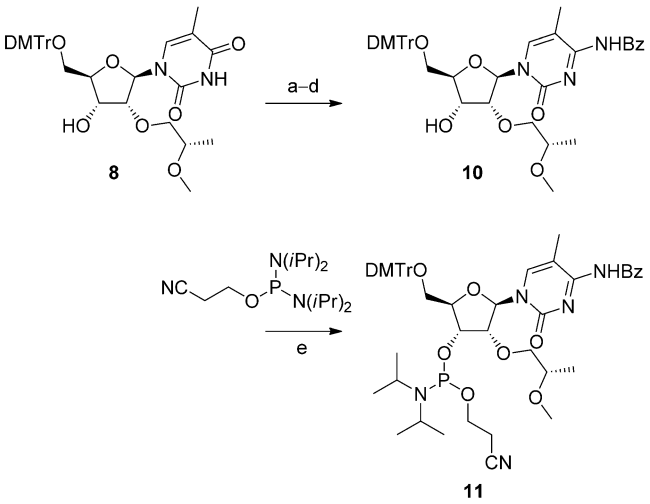

Scheme 2. Gram-scale synthesis of 2*S*-MOP 5-Me-cytidine phosphoramidite **11**. *Reagents and conditions*: a) Et_3N, TMSCl, MeCN, RT, 30 min; b) 1,2,4-triazole, $POCl_3$, 0 °C to RT, 1 h; c) Aq NH_3, RT, 12 h; d) Bz_2O, DMF, RT, 12 h (86%, four steps); e) *N*-methyl-imidazole (0.25 equiv), tetrazole (0.8 equiv), DMF, RT, 8 h, (85%).

The 3′-hydroxy group in **8** was first transiently protected as the trimethylsilyl (TMS) ether followed by reaction of the thymine nucleobase with phosphorus oxychloride and 1,2,4-triazole to provide the corresponding 4-triazolide. Displacement of the 4-triazolide with aqueous ammonia followed by protection of the exocyclic amino group as the benzoate ester provided the 5′-*O*-DMTr-protected 5-Me-cytosine nucleoside (**10**) in good yield. A phosphitylation reaction then provided the desired phosphoramidite (**11**).

Next, we evaluated the ability of 2*S*-MOP to stabilize oligonucleotide duplexes with complementary RNA in thermal denaturation experiments, and the results are given in Table 1.

Table 1. Duplex-stabilizing properties of 2′-*O*-methoxyethyl RNA (MOE)- and 2′-*O*-(2*S*-methoxypropyl)-RNA (2*S*-MOP)-modified oligonucleotides versus complementary RNA.

Oligonucleotide	Modification	Sequence (5′–3′)[a]	ΔT_m [°C][b]
A1	DNA	GCGTTTTTTGCG	control
A2	MOE	GCGT**TTTT**TGCG	+0.9
A3	2*S*-MOP	GCGT**TTTT**TGCG	+1.1
B1	DNA	CCAGTGATATGC	control
B2	MOE	CCAG**T**GA**T**A**T**GC	+1.7
B3	2*S*-MOP	CCAG**T**GA**T**A**T**GC	+1.9

[a] Base code—A = adenine, G = guanine, T = thymine, ^{m}C = 5-methyl cytosine; bold and/or underlined letters indicate modified nucleotides; [b] Change in T_m value relative to the appropriate control; values were measured in 10 mM sodium phosphate buffer (pH 7.2), containing 100 mM NaCl and 0.1 mM EDTA. Sequence of RNA complement 5′-r(AGCAAAAAACGC)-3′ for **A1**–**A3** and 5′-r(GCAUAUCACUGG)-3′ for **B1**–**B3**.

MOE (**2**) and 2*S*-MOP (**4**) nucleosides were incorporated into two oligonucleotide sequences (**A** and **B**) on an automated DNA synthesizer using standard phosphoramidite chemistry (Supporting Information). Evaluation of 2*S*-MOP-modified oligonucleotides **A3** (ΔT_m + 1.1 °C/mod.) and **B3** (ΔT_m + 1.9 °C/mod.) in T_m experiments revealed that the additional methyl group in the *S* configuration did not interfere with the ability of the modification to stabilize oligonucleotide duplexes in comparison with the corresponding MOE-modified oligonucleotides **A2** (ΔT_m + 0.9 °C/mod.) and **B2** (ΔT_m + 1.7 °C/mod.).

We prepared MOE, 2*S*-MOP and *S*-cEt gapmer ASOs **C1**, **C2** and **C3**, respectively (Table 2), targeting mouse scavenger receptor B1 (*Srb1*) mRNA for evaluation in animals. *Srb1* is ubiquitously expressed in all tissues, and ASOs targeting this mRNA have been used previously by us to profile oligonucleotide chemical modifications in animal experiments.[11] ASOs **C1** and **C2** were fully PS-modified 20-mers with a 10-base DNA gap region flanked on either end with five MOE or 2*S*-MOP nucleotides. For ASO **C2**, we used one incorporation of MOE-guanine at the 5′-end of the ASO because of unavailability of 2*S*-MOP-guanine phosphoramidite. ASO **C3** also had the same 10-base DNA gap as **C1** and **C2**, which is flanked on each side with two *S*-cEt nucleotides. The use of higher affinity *S*-cEt nucleotides permits the use of shorter ASOs, which at times can be more potent than longer ASOs.[9] The longer ASOs **C1** and **C2** showed higher duplex thermal stability as compared with the shorter ASO **C3** when paired with complementary RNA strands (Table 2).

Table 2. Sequence of antisense oligonucleotides (ASOs) targeting mouse scavenger receptor B1 (*Srb1*) and phosphatase and tensin homologue (*PTEN*) mRNA used for mouse experiment.

ASO	Modification	Target	Sequence (5′–3′)[a]	T_m [°C][b]
C1	MOE	*Srb1*	**G^{m}CTT^{m}C**AGT^{m}CATGA^{m}CT**T^{m}C^{m}CTT**	69.7
C2	2*S*-MOP	*Srb1*	**G^{m}CTT^{m}C**AGT^{m}CATGA^{m}CT**T^{m}C^{m}CTT**	69.0
C3	*S*-cEt	*Srb1*	**T^{m}C**AGT^{m}CATGA^{m}CT**T^{m}C**	59.0
D1	MOE	*PTEN*	**^{m}CTG^{m}CT**AG^{m}C^{m}CT^{m}CTGGA**TTTGA**	67.9
D2	2*S*-MOP	*PTEN*	**^{m}CTG^{m}CT**AG^{m}C^{m}CT^{m}CTGGA**TTTGA**	67.1
D3	*S*-cEt	*PTEN*	**^{m}CT**TAGCACTGGC**^{m}CT**	62.2

[a] Base code—A = adenine, G = guanine, T = thymine, ^{m}C = 5-methyl cytosine; bold and/or underlined letters indicate modified nucleotides; [b] T_m values were measured in 10 mM sodium phosphate buffer (pH 7.2) containing 100 mM NaCl and 0.1 mM EDTA using complementary RNA.

ASOs **C1**, **C2** and **C3** were evaluated in an animal experiment for their ability to inhibit *Srb1* mRNA expression in liver, diaphragm, quadricep, and gastrocnemius muscle. Balb-c mice were injected subcutaneously twice weekly for three weeks with ASOs **C1**, **C2** and **C3** (25 mg kg^{-1}). The animals were then sacrificed 72 hours after the last dose, the liver, quadricep, gastrocnemius, and diaphragm tissues were collected, homogenized and analyzed for changes in *Srb1* mRNA levels as compared with saline-treated controls. Plasma transaminase levels and organ weights were also recorded after sacrifice to assess tolerability. ASOs **C1** and **C2** showed excellent activity for decreasing *Srb1* mRNA in liver and diaphragm, but reduced activity in quadriceps, heart, and gastrocnemius muscle. In contrast, the shorter ASO (**C3**) showed excellent activity in all tissues examined (Figure 3a). All ASOs were well tolerated with no adverse effects on plasma alanine transaminase (ALT) and blood urea nitrogen (BUN) levels, or organ and body weights (Figure 3b–d).

To examine whether 2*S*-MOP could enhance activity in muscle for a different sequence or target, we investigated ASOs **D1**, **D2** and **D3** targeting another ubiquitously expressed gene, phosphatase and tensin homologue (*PTEN*).[17] Balb-C mice were injected subcutaneously with ASOs **D1** and **D2** (50 mg kg^{-1}) and **D3** (25 mg kg^{-1}) twice weekly for three weeks. Animals were sacrificed 72 hours after the last dose, and liver, quadricep, gastrocnemius and diaphragm tissues were collected, homogenized and analyzed for changes in phosphatase and tensin homologue (*PTEN*) mRNA levels as compared with saline-treated controls. Plasma transaminase levels and organ weights were recorded after sacrifice to assess tolerability. We observed a greater than 90% decrease in *PTEN* mRNA in liver for all ASOs. However, 2S-MOP-modified ASO **D2** showed better activity in diaphragm (* $p < 0.0286$) and quadricep (ns = not significant) as compared with the corresponding MOE-modified ASO, **D1**. In contrast, **D1** showed better downregulation of *PTEN* in gastrocnemius (* $p < 0.0286$)

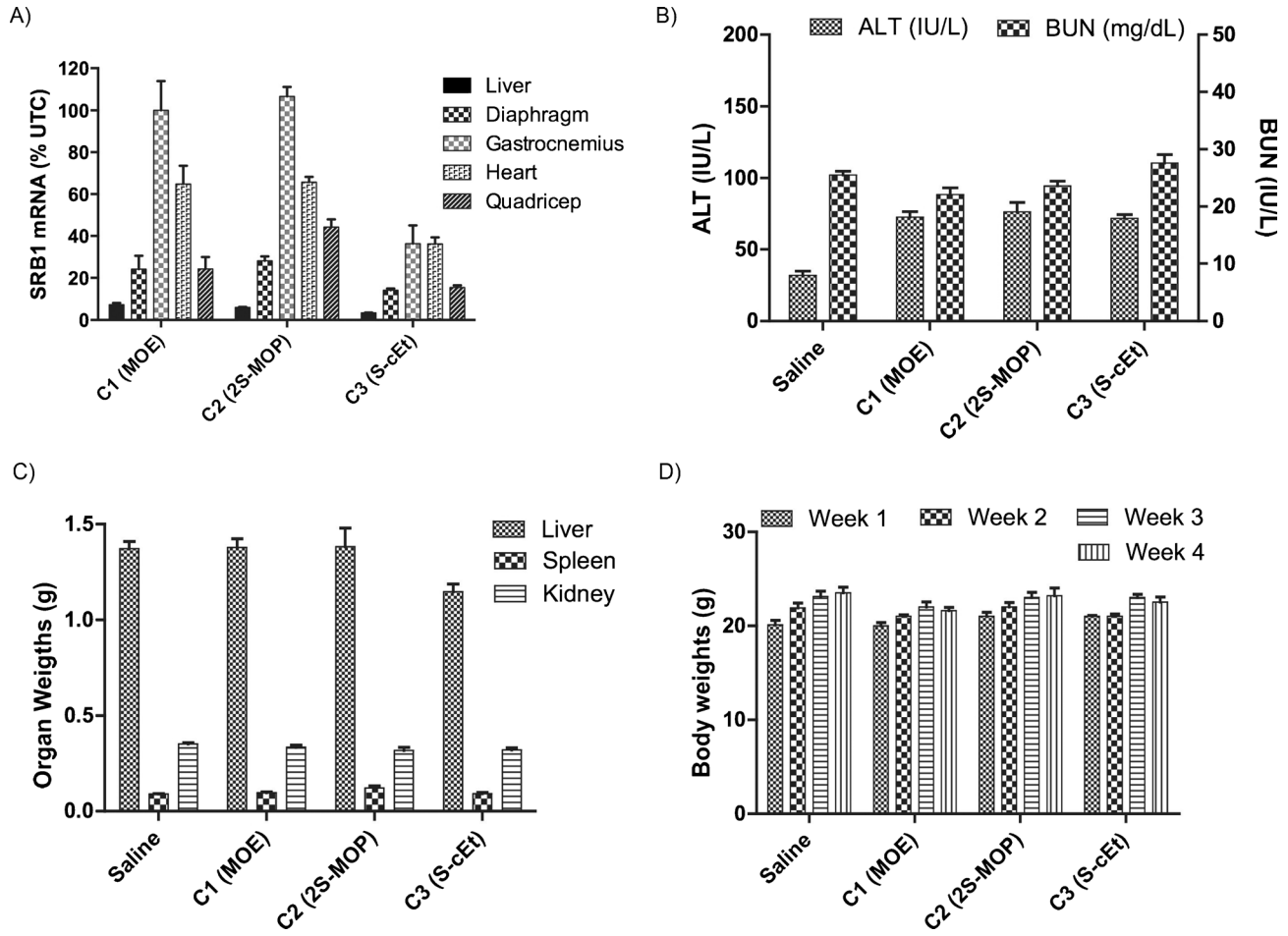

Figure 3. Summary of activity and tolerability data for MOE, 2*S*-MOP and *S*-cEt antisense oligonucleotides (ASOs) targeting mouse *Srb1*. Mice (Balb-C, $n=4$/group) were injected subcutaneously with ASOs **C1**, **C2** and **C3** (25 mg kg^{-1} twice a week for three weeks) targeting mouse scavenger receptor B1 (*Srb1*). The mice were sacrificed 72 h after the last ASO dose, tissues were collected and weighed, and plasma chemistries were recorded. A) Selected tissues were homogenized and analyzed for the change in *Srb1* mRNA content relative to saline-treated controls. B) Alanine transaminase (ALT) and blood urea nitrogen (BUN) levels and C) organ weights were recorded post-sacrifice. D) Body weights during the three-week study showing minimal differences from saline-treated groups. All data are expressed as mean ± SEM.

and heart (*$p < 0.0286$). In general, **D1** and **D2** showed activity comparable with **D3** in all tissues tested. However, unlike the *Srb1* study where ASOs **C1**, **C2** and **C3** were dosed at 25 mg kg^{-1}/twice weekly for three weeks, **D1** and **D2** were dosed at 50 mg kg^{-1} while **D3** was dosed at 25 mg kg^{-1} twice weekly for three weeks. All ASOs were well tolerated with no changes in organ weights (Figure 4b) or other parameters of tolerability.

In summary, we report the synthesis and antisense activity of a hydrophobic MOE RNA analogue for antisense applications. In general, the increased hydrophobicity imparted by the 2*S*-MOP modification did not translate to improved activity in all extrahepatic tissues as compared with the parent MOE ASOs. However, we did observe improved activity in diaphragm and quadricep muscle for the 2*S*-MOP ASO **D2** targeting mouse *PTEN*, suggesting that sequence and target may play some role in determining ASO activity in muscle. Interestingly, the shorter cEt ASOs generally showed the best activity in multiple extrahepatic tissues. Presumably, the lower molecular weight and decreased charge facilitates more efficient release of shorter ASOs from endosomal and lysosomal compartments. Our data further highlight the complex interplay between ASO length, modification pattern, PS content, and overall charge for activity in animal experiments.

Experimental Section

Experimental procedures for preparing phosphoramidites **9** and **11** from compound **5**, oligonucleotide synthesis, T_m measurements, and methods for the animal experiments are provided in the Supporting Information, available via http://dx.doi.org/10.1002/cmdc.201402099.

For in vivo experiments, the Institutional Animal Care and Use Committee (IACUC) approved all procedures.

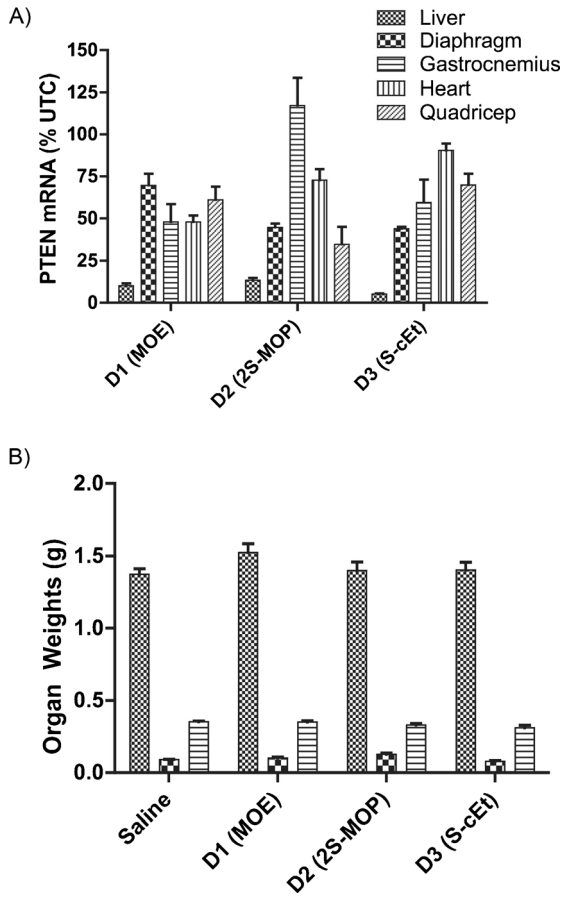

Figure 4. Summary of activity and tolerability data for MOE, 2*S*-MOP and *S*-cEt antisense oligonucleotides (ASOs) targeting mouse *PTEN*. Mice (Balb-C, $n=4$/group) were injected subcutaneously with ASOs **D1**, **D2** (50 mg kg^{-1}) and **D3** (25 mg kg^{-1}) targeting mouse *PTEN*, twice a week for three weeks. The mice were sacrificed 72 h after the last ASO dose, and tissues were collected and weighed. A) Selected tissues were homogenized and analyzed for the change in *PTEN* mRNA content relative to saline-treated controls. B) Organ weights were recorded post-sacrifice. All data are expressed as mean ± SEM.

Keywords: antisense oligonucleotides · gapmers · methoxyethyl RNA derivatives · methylation

[1] H. Wu, W. F. Lima, S. T. Crooke, *J. Biol. Chem.* **1999**, *274*, 28270 – 28278.
[2] C. F. Bennett, E. E. Swayze, *Annu. Rev. Pharmacol. Toxicol.* **2010**, *50*, 259 – 293.
[3] F. Eckstein, *Antisense Nucleic Acid Drug Dev.* **2000**, *10*, 117 – 121.
[4] P. Martin, *Helv. Chim. Acta* **1995**, *78*, 486 – 504.
[5] R. S. Geary, *Expert Opin. Drug Metab. Toxicol.* **2009**, *5*, 381 – 391.
[6] C. F. Bennett in *Antisense Drug Technology: Principles, Strategies and Applications, 2nd ed.* (Ed.: S. T. Crooke), CRC Press, Boca Raton, **2007**, pp. 273 – 304.
[7] R. G. Lee, J. Crosby, B. F. Baker, M. J. Graham, R. M. Crooke, *J. Cardiovasc. Transl. Res.* **2013**, *6*, 969 – 980.
[8] T. M. Wheeler, A. J. Leger, S. K. Pandey, A. R. MacLeod, M. Nakamori, S. H. Cheng, B. M. Wentworth, C. F. Bennett, C. A. Thornton, *Nature* **2012**, *488*, 111 – 115.
[9] P. P. Seth, A. Siwkowski, C. R. Allerson, G. Vasquez, S. Lee, T. P. Prakash, E. V. Wancewicz, D. Witchell, E. E. Swayze, *J. Med. Chem.* **2009**, *52*, 10 – 13.
[10] D. Renneberg, C. J. Leumann, *J. Am. Chem. Soc.* **2002**, *124*, 5993 – 6002.
[11] S. Murray, D. Ittig, E. Koller, A. Berdeja, A. Chappell, T. P. Prakash, M. Norrbom, E. E. Swayze, C. J. Leumann, P. P. Seth, *Nucleic Acids Res.* **2012**, *40*, 6135 – 6143.
[12] M. Teplova, G. Minasov, V. Tereshko, G. B. Inamati, P. D. Cook, M. Manoharan, M. Egli, *Nat. Struct. Biol.* **1999**, *6*, 535 – 539.
[13] S. P. Henry, T.-W. Kim, K. Kramer-Strickland, T. A. Zanardi, R. A. Fey, A. A. Levin in *Antisense Drug Technology: Principles, Strategies and Applications, 2nd ed.* (Ed.: S. T. Crooke), CRC Press, Boca Raton, **2007**, pp. 327 – 364.
[14] V. Kotikam, V. A. Kumar, *Tetrahedron* **2013**, *69*, 6404 – 6408.
[15] B. S. Ross, Q. Song, M. Han, *Nucleosides Nucleotides Nucleic Acids* **2005**, *24*, 815 – 818.
[16] P. P. Seth, G. Vasquez, C. A. Allerson, A. Berdeja, H. Gaus, G. A. Kinberger, T. P. Prakash, M. T. Migawa, B. Bhat, E. E. Swayze, *J. Org. Chem.* **2010**, *75*, 1569 – 1581.
[17] M. Butler, R. A. McKay, I. J. Popoff, W. A. Gaarde, D. Witchell, S. F. Murray, N. M. Dean, S. Bhanot, B. P. Monia, *Diabetes* **2002**, *51*, 1028 – 1034.

Received: April 1, 2014
Published online on May 28, 2014